Enhancing Cisplatin Anticancer Effectivity and Migrastatic Potential by Modulation of Molecular Weight of Oxidized Dextran Carrier

L. Münster,[1] M. Fojtů,[2,3,4] M. Muchová,[1] F. Latečka,[1] S. Káčerová,[1] Z. Capáková,[1] T. Juriňáková[2,4], I. Kuřitka,[1] M. Masařík,[2,3,4,5]* J. Vícha[1]*

[1]*Centre of Polymer Systems, Tomas Bata University in Zlín, tř. Tomáše Bati 5678, 760 01 Zlín, Czech Republic*

[2]*Department of Physiology, Faculty of Medicine, Masaryk University, Kamenice 5, CZ-625 00 Brno, Czech Republic*

[3]*Center for Advanced Functional Nanorobots, Department of Inorganic Chemistry, Faculty of Chemical Technology, University of Chemistry and Technology in Prague, Technická 5, Prague CZ-166 28, Czech Republic*

[4]*Department of Pathological Physiology, Faculty of Medicine, Masaryk University, Kamenice 5, CZ-625 00 Brno, Czech Republic*

[5]*BIOCEV, First Faculty of Medicine, Charles University, Průmyslová 595, 252 50, Vestec, Czech Republic*

Emails: jvicha@utb.cz, masarik@med.muni.cz

Abstract: The molecular weight (M_w) of dextran derivatives, such as regioselectively oxidized dicarboxydextran (DXA), is greatly influencing their faith in an organism, which could be possibly used to improve anticancer drug delivery. Here we present a modified method of sulfonation-induced chain scission method allowing direct and accurate control over the M_w of DXA without increasing its polydispersity. Prepared DXA derivatives (M_w = 10–185 kDa) have been conjugated to cisplatin and the M_w of the carrier found to have a significant impact on cisplatin release rates, *in vitro* cytotoxicity, and migrastatic potential. Conjugates with the high-M_w DXA showed particularly increased anticancer efficacy. The best conjugate was four times more effective against malignant prostatic cell lines than free cisplatin and significantly inhibited the ovarian cancer cell migration. This was traced to the characteristics of spontaneously formed cisplatin-crosslinked DXA nanogels influenced by M_w of DXA and cisplatin loading.

Keywords: drug-delivery; dextran; periodate oxidation; molecular weight; cisplatin; carrier;

1. Introduction

Over the last several decades, intensive efforts have been made to design and develop advanced drug delivery systems which would improve the targeting and effectivity of platinum anticancer drugs such as cisplatin, *cis*-$[Pt(NH_3)_2Cl_2]$. Glycoconjugation of platinum anticancer drugs to various carbohydrates has been shown to improve their anticancer efficacy and targeting of malignancies due to the increased requirements of cancer cells for carbohydrates (Warburg effect). (Annunziata, Amoresano, et al., 2020; Annunziata, Cucciolito, et al., 2020; Bononi et al., 2021) Conjugation of platinum anticancer drugs to polysaccharides prolongs the circulation time of the drug in the blood, reduces its systemic toxicity, and improves its passive accumulation in the tumor due to the enhanced permeability and retention (EPR) effect. (Haxton & Burt, 2009; Liechty et al., 2010; Vilar et al., 2012)

Dextrans are α-(1→6) bonded glucans produced by *Leuconostoc* and *Streptococcus* genus of bacteria with a variable degree of α-(1→3) branching, which, together with their molecular weight, depends not only on the bacterial genus but also on its strain. (Dhaneshwar et al., 2006; Sarwat et al., 2008) Since the 1950s, dextrans have been used in clinical praxis as plasma volume expanders, for blood flow promotion, or as antithrombotic agents. (Thorén, 1980) The plasma kinetics, renal clearance, the rate of degradation, and tissue distribution of dextrans were thus intensively studied and found to depend on the molecular weight as well as on the charge and the degree of substitution of the dextran chains. (Goodarzi et al., 2013; Mehvar, 2000, 2003; Varshosaz, 2012) The impact of molecular weight is particularly pronounced; dextrans with weight-average molecular weight (M_w) below 10 kDa are rapidly eliminated from the organism because of their very high rate of renal clearance. (Chang et al., 1975) Higher molecular weight dextrans (M_w > 70 kDa) spontaneously accumulate in the liver and spleen, where they can persist up to 96 h before being metabolized. (Mehvar et al., 1994) High-M_w dextrans (M_w > 150 kDa) also tend to accumulate in the lymph nodes to a significant degree. (Terry et al., 1953) The ratio of dextran accumulation between individual organs and tissues thus largely depends on its M_w. (Mehvar et al., 1994) These properties make dextran derivatives potentially very interesting as an anticancer drugs carrier because the liver and lymphatic nodes are often among the first tissues invaded by metastases and thus represent the primary target for chemotherapy. Hypothetically, obtaining control over the molecular weight of dextran derivatives may significantly enhance their drug delivery characteristics and thus improve the efficacy of anticancer drugs.

Over the years, dextran and its derivatives had been intensively studied as anticancer drug carriers. (Dhaneshwar et al., 2006; Goodarzi et al., 2013; Schechter, Neumann, et al., 1989; Varshosaz, 2012) Modification of dextran for anticancer drug binding is often achieved by the introduction of carboxylic groups to the polysaccharide chain. Advantageously, such negatively charged dextran derivatives persist in plasma much longer than neutral or positively charged ones, (Mehvar, 2000) which may enhance the EPR effect because the carrier has more time to accumulate in the tumor due to the leaky vasculature. This is attributed to the negative charge of most biological membranes, which impede the uptake of molecules with the same charge, thus prolonging their residence in the vascular system. (Mehvar, 2000) Chemical modifications of dextran chains were also reported to improve their overall stability in the body, *i.e.* while unmodified dextrans are depolymerized by α-1-glucosidases (dextranases) in few hours, any modification would generally reduce the rate of depolymerization. (Mehvar, 2000) For instance,

periodate-oxidized dextran derivatives with a degree of oxidation (*DO*) above 90 % were shown to be largely resistant to dextranase hydrolysis. (Ahmad et al., 2006)

Modification of dextran for binding of platinum drugs can be achieved for instance by sequential oxidation of vicinal –OH groups of anhydroglucose units (AGU) to aldehydes by periodate and subsequent oxidation of formed aldehydes to carboxylates by chlorite salt, which leads to the preparation of a mixture of 2,4- and 3,4-dicarboxydextrans (Ishak & Painter, 1978; Khomyakov et al., 1965; Kristiansen et al., 2010) collectively referred to as DXA in this work, see Figure 1. The third potential product, 2,3-dicarboxydextran, is significantly less abundant (Khomyakov et al., 1965) and was not observed in NMR spectra of DXA.(Münster et al., 2021) Hence, it is not further discussed. Note, that the periodate oxidation requires two –OH groups on neighboring (vicinal) carbons, which are oxidized simultaneously. Hence, branched DXA units are resistant to oxidation as they do not contain required vicinal diols because their –OH groups at C1, C3, and C6 engaged in glycosidic bonds (Figure 1). (Khomyakov et al., 1965; Kristiansen et al., 2010)

Other methods of derivatization of dextran chain include carboxymethylation or dicarboxymethylation of dextran –OH groups resulting in the preparation of carboxymethyl dextran (CMD) or dicarboxymethyl dextran (DMD), respectively. (Ohya et al., 1996b; Schechter et al., 1986)

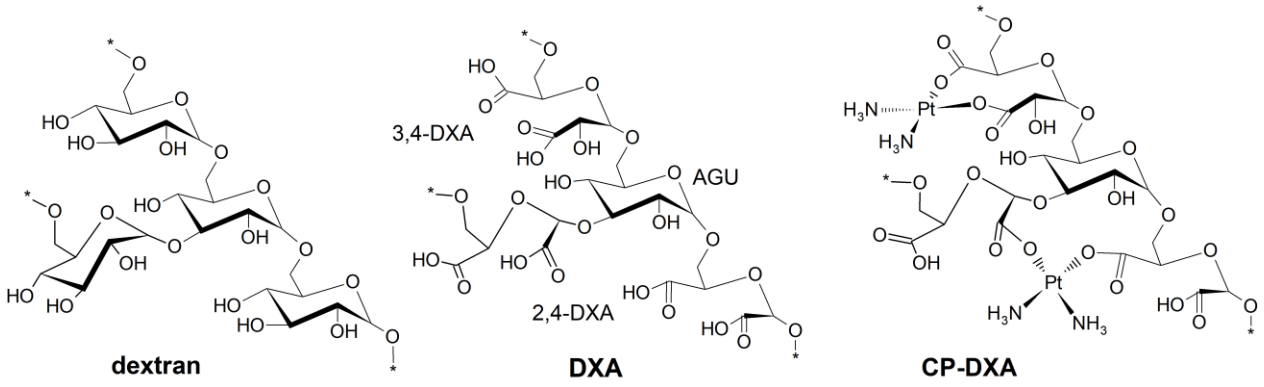

Figure 1 Structure of dextran and 2,4- and 3,4-oxidized dextran (DXA) prepared by sequential periodate-chlorite oxidation; structure of cisplatin-DXA (CP-DXA) conjugate showing two main binding modes of CP, i.e. the bidentate binding of CP in single DXA unit and CP crosslinking of nearby oxidized DXA units. (Münster et al., 2021)

Schlechter et al. studied the synthesis,(Schechter et al., 1986) biological activity (Schechter et al., 1987), and blood levels (Schechter, Rosing, et al., 1989) of CMD conjugates with CP. Although the studied CP-CMD conjugates (M_w = 10 and 40 kDa) did not differ in their *in vitro* activity, both being less cytotoxic than free CP, *in vivo* tests revealed that both conjugates had higher plasma concentrations and longer half-lives than the free drug, depending on their M_w. While the content of free CP in mouse serum decreased to only 2-6% of its initial concentration already after 15 min since the i.v. administration, 14% of 10 kDa CP-CMD and 64% of 40 kDa CP-CMD conjugate remained after the same time. Even after six hours, about 11% of 40 kDa CP-CMD was still detected in the serum. (Schechter, Rosing, et al., 1989) In the same work, Schechter et al. investigated also CMD with M_w = 250 kDa, which was found to retain the blood levels of platinum drug the longest (100% after 15 min, 47% after 100 min, and 14% after 6 h).

Later on, Ohya *et* al. compared DXA, CMD, and DMD as carriers for a derivative of oxaliplatin. (Ohya et al., 1996b, 1996a) Both DXA and DMD-based conjugates were found superior to CMD one; their cytotoxicity against malignant cells was higher (comparable with a free drug) and they showed a lower decrease of cytotoxic activity after the pre-incubation in a medium containing fetal bovine serum. The DXA and DMD carriers thus provided better protection of the carried drug from the deactivating factors in serum than CMD, likely due to bidentate binding of the complex to the carrier. (Ohya et al., 1996a) In follow-up work, Nakashima *et* al. (Nakashima et al., 1999) compared the DMD and DXA with identical M_w of 30 kDa as carriers for CP. Although CP-DXA conjugate showed higher cytotoxic activity, the cytotoxicity of CP-DMD was better retained after 36 h of pre-incubation in the presence of fetal bovine serum. Observed faster loss of activity of CP-DXA might however be a result of considerably higher platinum content (22 wt%) in CP-DXA compared to CP-DMD (9 wt%), which led to a faster release of the drug from the former. Recently, we have included DXA (M_w = 87 kDa) in the comparison of selectively oxidized polysaccharides as carriers for CP, (Münster et al., 2021) established structures of CP-DXA conjugate are given in Figure 1. Despite certain drawbacks, in particular the fast drug release rates in comparison to other carriers, DXA was deemed to be a potentially interesting carrier for CP given the highest overall cellular uptake and high cytotoxicity towards malignant cell lines, comparable or better to that of free drug (depending on the cell line). The CP-DXA also featured the lowest cytotoxicity towards non-cancerous cell line NIH/3T3 from all anhydroglucose-based carriers, including the oxidized cellulose and oxidized dextrin. Encouraged by these results, we have decided to investigate DXAs with different M_w as carriers for CP and to identify possible benefits and drawbacks related to the modulation of its M_w.

Hence, the recently developed method for direct control over the M_w of selectively oxidized polysaccharides with 1-4 glycosidic bonds(Münster, Fojtů, et al., 2019; Münster et al., 2020) was modified to prepare series of DXA derivatives with a broad range of M_w (10 – 184 kDa). Subsequently, prepared dextran derivatives were characterized by FT-IR, GPC, and NMR spectroscopies and loaded with different amounts of CP (15, 30, and 45 wt%). Dependence of drug release rates, *in vitro* cytotoxicity, and migrastatic potential on M_w of CP-DXA conjugates have been investigated and results compared to the free CP. CP was selected as a model drug because it is currently still used as a first-line drug for the therapy of patients diagnosed with lung, ovarian, cervix, bladder, testicular, or head and neck cancer. As a first-generation platinum chemotherapeutic, it also causes adverse side effects such as nausea, neurotoxicity, nephrotoxicity, and ototoxicity, mostly due to its non-specific mechanisms of action and cumulation in healthy tissues. Conjugation of CP to DXA with variable M_w should provide better organ/tumor targeting, thus reducing its off-target toxicity. Conjugation should also protect the drug during its transport in the vascular system and prevents its reactions with various targets of opportunity, such as thiol-containing proteins. Besides, conjugation to macromolecular carriers allows CP to avoid renal clearance, increase its plasma half-life, and accumulate in the tumor (EPR effect).

2. Materials and Methods

2.1 Materials. Dextran from *Leuconostoc spp.* (Sigma Aldrich Co., M_w = 106 kDa, *PDI* = 5.59, estimated by GPC using setup described in section *2.3*) was used as a source polysaccharide. The primary oxidation was performed by sodium periodate ($NaIO_4$) and ethylene glycol (Penta, Czech Republic). The secondary oxidation of dialdehyde polysaccharides was carried out using sodium chlorite ($NaClO_2$, RT 80 %), acetic

acid (CH_3COOH, ≥99.8 %), sulfamic acid (H_3NSO_3, 99.3 %) (Sigma Aldrich, Co.), sodium hydroxide (NaOH, ≥98 %) (Lachner, Czech Republic) and hydrochloric acid (HCl, 35 %) (Penta, Czech Republic). Other chemicals involved in the characterization of source and resulting materials included sodium nitrate ($NaNO_3$, 99.8 %) (Lachner, Czech Republic), disodium phosphate dodecahydrate ($Na_2HPO_4 \cdot 12H_2O$, 99.6 %) (VWR, Czech Republic), deuterium oxide (D_2O, Sigma Aldrich, Co.) and phosphate-buffered saline pH 7.4 (PBS 7.4, Invitrogen, USA). Reagents used for the biological experiments included RPMI-1640 medium, fetal bovine serum (FBS) (mycoplasma-free), penicillin-streptomycin, trypsin, MTT reagent, ethylenediaminetetraacetic acid (EDTA), dimethyl sulfoxide (DMSO), glycine buffer, and hydroxyethyl-piperazine-ethane-sulfonic acid buffer (HEPES) (Merck, Germany). All chemicals were of analytical grade and were used without further purification. Demineralized water (conductivity >0.1 µS/cm) was used throughout the experiments.

2.2 Preparation of DXA with variable M_w. The first step of dextran selective oxidation follows well-established methods of periodate oxidation.(Khomyakov et al., 1965; Münster et al., 2021; Maia et al., 2011; Münster et al., 2017; Münster, Capáková, et al., 2019) Briefly, 5 g of dextran was pre-dissolved for 1 h in 150 mL of water at laboratory temperature. Then, 8.25 g of $NaIO_4$ dissolved in 100 mL of water was added dropwise to the solution. The primary oxidation ran at 30 °C for 4 h under mild stirring (300 rpm) in the dark to prevent spontaneous periodate decomposition. The duration of primary oxidation was previously optimized based on periodate consumption estimated by UV-Vis spectroscopy(Münster et al., 2021) and it is sufficient to obtain fully oxidized dextran chains. After this period, the oxidation reaction was terminated by the addition of an excess of ethylene glycol. The prepared dialdehydedextran was then dialyzed against demineralized water using 14 kDa molecular weight cut-off (*MWCO*) dialysis tubing (Sigma Aldrich, Co.) for 4 days with regular water exchange. Next, the product was collected, filtered (0.22 µm filter), flash-frozen at -80 °C using an ethanol ice bath, and lyophilized.

The second step of DXA preparation involves oxidation of dialdehydedextran by $NaClO_2$ in the presence of CH_3COOH. The reaction mixture was composed of 0.45 g of the prepared dialdehydedextran, which was dissolved in 45 mL of 0.5 M CH_3COOH. The secondary oxidation started by dropwise addition of concentrated $NaClO_2$ solution (0.25 g/mL) to the acidified dialdehydedextran solution (final concentration 0.5 M). The molar ratio of –CHO : $NaClO_2$ was set to 1:4. The mixture was gently stirred for 7 h at laboratory temperature in the dark. After this period, the oxidation reaction was terminated by the addition of a concentrated NaOH solution (pH = 8). Then, the product solution was thoroughly dialyzed against water using a 14 kDa *MWCO* dialysis membrane. Diluted (0.1 M) NaOH and HCl solutions were then used to set the pH of the solution to 7.4. The resulting purified dicarboxydextran sodium salt (DXA) solution was filtered (0.22 µm filter), flash-frozen, and lyophilized.

To prepare DXA of various M_w, sulfonation-induced scission was initiated by the addition of sulfamic acid into the reaction mixture before the secondary oxidation to control the M_w of the final product. (Münster et al., 2020; Münster, Fojtů, et al., 2019) In the first set of experiments, the standard protocol of sulfonation-induced scission used previously for M_w modulation of cellulose and dextrin was employed, *i.e.* H_3NSO_3 (0.11 g/mL) was added to the dialdehydedextran solutions immediately before the start of the secondary oxidation by the addition of $NaClO_2$.(Münster et al., 2020; Münster, Fojtů, et al., 2019) Different molar ratios of –CHO : H_3NSO_3 (from 1:0 to 1:0.5) were tested. The rest of the process parameters and

methodology of secondary oxidation remained the same as described in the previous paragraph. Because of unsatisfactory results, a modified methodology featuring a presulfonation step of various lengths was used in the second set of experiments. Briefly, the solution of H_3NSO_3 was added dropwise to the set of acidified dialdehydedextran sample solutions (molar ratio of –CHO : H_3NSO_3 set to 1:0.5, final H_3NSO_3 concentration was 0.0625 M) prior to the start of the secondary oxidation as before. However, these reaction mixtures were stirred for 0.5–6 h (*i.e.* presulfonation step) before the initiation of secondary oxidation by $NaClO_2$ solution addition. Subsequent steps in the preparation methodology remained the same as above. All of the DXA samples were prepared in the form of their sodium salt. Results are discussed in Section *3.1*.

2.3 Characterization of prepared DXA. Spectral FT-IR analysis was performed using a Nicolet 6700 (Thermo Scientific, USA). Spectra were collected in the range of 4000–400 cm^{-1} with 64 scans and a resolution of 2 cm^{-1} with atmosphere gas suppression enabled. Energy dispersive spectroscopic (EDS) analysis of prepared samples was conducted by using scanning electron microscope Vega II/LMU (Tescan, Czech Republic) operated at 30 keV equipped with energy dispersive X-Ray (EDX) detector Inca X-act (Oxford Instruments, UK). Molecular weight distribution was analyzed by the gel permeation chromatography (GPC) using a Waters HPLC Breeze chromatographic system (Waters, USA) coupled with a Waters 2414 refractive index detector (drift tube T = 60 °C), Tosoh TSK gel $GMPW_{XL}$ column (300 mm×7.8 mm×13 µm, column T = 30 °C). A mixture of 0.1 M $NaNO_3$ and 0.05 M $Na_2HPO_4 \cdot 12\ H_2O$ was used as a mobile phase. A calibration kit of pullulan standards SAC-10 (Agilent Technologies, USA) in a span of M_w 342–805 000 g/mol was employed. ^1H NMR spectra were measured using Bruker Avance III HD 700 MHz NMR spectrometer (Bruker, USA) equipped with a triple-resonance cryoprobe at 298 K in D_2O.

2.4 Preparation and characterization of cisplatin-DXA conjugates. CP was prepared according to the literature. (Wilson & Lippard, 2014) It was then dissolved in water (2 mg/mL) and added dropwise to the 4 mg/mL aqueous solution of the DXA at room temperature. The reaction mixture was then gently shaken for 72 h in the absence of light, dialyzed against water for 4 h using a 3.5 kDa *MWCO* membrane to remove unbound CP, filtered, and lyophilized. Reactions were performed using CP : carrier w/w loading ratio of 2:10, 5:10, and 8:10, respectively. CP release was investigated using a setup mimicking *in vitro* conditions;(Münster, Fojtů, et al., 2019) 10 mg of each conjugate was dissolved at 37 °C in 5 mL of PBS 7.4 and dialyzed (3.5 kDa *MWCO* membrane) against 95 mL of the same medium. Aliquots of 5 mL were collected throughout 48 h and replaced with 5 mL of fresh media to conserve the volume. Released cisplatin residuum, *cis*-$[Pt(NH_3)_2(H_2O)_2]^{2+}$ is in the following text also referred to as cisplatin (CP) to simplify the discussion. The amount of bonded platinum was measured by the energy-dispersive X-ray fluorescence (XRF) spectrometer ARL Quant'X EDXRF Analyzer (Thermo Scientific, USA) using the calibration standards prepared by dissolving a known amount of CP in PBS 7.4. The morphology of selected CP-DXA conjugates was analyzed by transmission electron microscopy (TEM) using JEM 2100 microscope (Jeol, Japan) operated at 160 kV. Samples were drop-cast onto Formvar coated 300 mesh copper grids from diluted solution (0.01 mg/mL) and gently dried. The stability (ζ-potential) and hydrodynamic radius of selected diluted samples (1 mg/mL) were analyzed by dynamic light scattering (DLS) analysis carried out using Zetasizer Nano ZS90 instrument (Malvern Instruments, UK) operated at 25 °C, coupled with DTS1070 cells and the Smoluchowski model.

2.5 Cytotoxicity evaluation. Six tumor cell lines originating from different tissues were used in this study: i) A2780 - epithelial ovarian cancer cells established from tumor tissue of an untreated patient and ii) corresponding CP-resistant subline A2780/CP, iii) A549 - human cell line derived from pulmonary adenocarcinoma, iv) 22Rv1 - cell line representing human prostate carcinoma, and v) PC-3 - human prostate cancer cell line established from bone metastasis. Cell lines were purchased from the European Collection of Authenticated Cell Cultures (ECACC, UK) and were cultivated in RPMI-1640 medium, supplemented with 10 % FBS, antibiotics (penicillin 100 U/mL and streptomycin 0.1 mg/mL), and HEPES. The cells were grown in the incubator at 37 °C in a humidified 5 % CO_2 mixture with ambient air and subsequently seeded on a 96-well plate at a density ensuring 70 % confluence on the day of the treatment. After 48 h, the medium was removed and replaced with a fresh culture medium containing CP-DXA conjugates in the concentration ranging from 0–500 µM (200 µL per well). After 24 and 48 h of the treatment, the cell culture medium with CP-carrier conjugates was removed and the cells were incubated with a fresh medium containing 1 mg/mL of MTT reagent (200 µL per well) for another 4 h. Plates with the cells were wrapped in aluminum foil and kept in a humidified atmosphere at 37 °C. Next, the culture medium with MTT was replaced by DMSO (200 µL per well) to dissolve the formazan crystals. Then, glycine buffer (25 µL per well) was added to DMSO, gently shaken and the absorbance value at 570 nm was recorded. Cytation 3 Imaging reader (BioTek Instruments, USA) was used for the determination of absorbance values. The IC_{50} values were then calculated by fitting the data with the logistic function to create a sigmoidal dose-response curve. All measurements were performed in tetraplicates.

2.6 Migration assay. A2780 cells were seeded on the tissue culture dishes at a density 2×10^5 per mL of media and incubated until they reached a confluent monolayer, which was then scratched using a sterile 200 µL pipette tip. The cellular debris was removed by washing with PBS five times and images of scratches were acquired. Subsequently, a medium containing selected samples in concentrations corresponding to their respective IC_{50} (established by MTT, see Section *2.5*) was added to the cells. Cells in Petri dishes were placed in the incubator, kept at 37 °C, examined periodically and images were taken at the same position after 24 and 48 h using the phase-contrast Olympus IX81 microscope (Olympus, Japan). The results were analyzed using T-Scratch software (CSElab, Zurich, Switzerland) and are presented as a percentage of open wound area remained after 24 and 48 h.

3. Results and discussion

3.1 Synthesis and characterization of DXA with a different molecular weight

Sequential oxidation of dextran from *Leuconostoc spp.* was performed as described in Section *2.2*. The yield of primary oxidation was nearly quantitative (96.7 %); the yields of all secondary oxidations were above 90 %.

The original method of sulfonation-induced chain scission, which relies on the addition of different amounts of sulfamic acid (H_3NSO_3) just before the secondary oxidation,(Münster et al., 2020; Münster, Fojtů, et al., 2019) was initially tested to prepare DXA derivatives with different M_w. It is based on the addition of acidic $–SO_3H$ groups to aldehydes introduced during the periodate oxidation. Attached $–SO_3H$ groups can efficiently protonate nearby glycosidic bonds, thus initiating their acidic hydrolysis. The $–SO_3H$ groups are eliminated during the oxidation of aldehydes to carboxylates, see ref. (Münster et al., 2020) for

the detailed reaction mechanism. This approach allows the preparation of dicarboxylated polysaccharides with different M_w using the same starting material. It can be also used to decrease the polydispersity index (*PDI*) of products compared to source polysaccharide. (Münster et al., 2020; Münster, Fojtů, et al., 2019) This saves resources and provides better control over the results than alternative approaches based on the oxidation of different source materials with various molecular weights or thermal degradation of prepared dicarboxylated polysaccharides, both of which offer only limited (if any) control over the M_w and *PDI* of the products.

However, the original method, developed for β-(1→4) bonded polysaccharides (namely cellulose), was found to be unsuitable for dextran (see Figure 3.1A and Table S1). The addition of H_3NSO_3 up to 0.25 M concentration had virtually no impact on the M_w of DXA, which started to decrease only in a presence of 0.5 M H_3NSO_3. The likely reason lies in the structure of DXA, which is formed mostly by 2,4- and 3,4-oxidized units connected by α-(1→6) glycosidic bonds. The $–SO_3H$ groups attached to C3 and C4 are thus relatively distant from α-(1→6) linkages and only sulfonation at C2 can lead to their effective protonation, see Scheme 1 for the reaction mechanism. This slows down the kinetics of the chain scission for DXA in comparison to β-(1→4) bonded cellulose units.

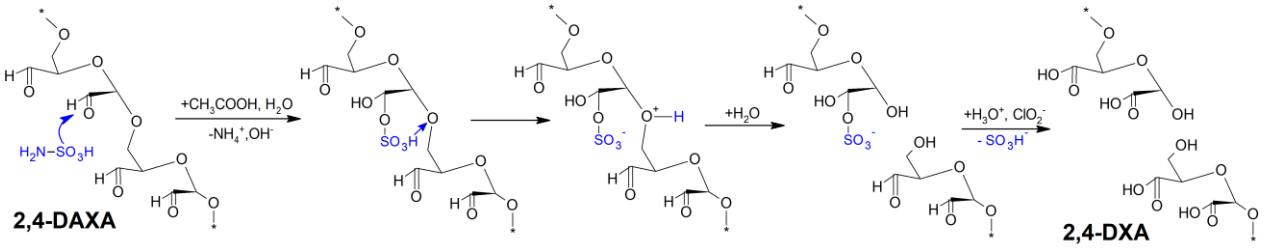

Scheme 1: Mechanism of sulfonation-induced chain scission on the example of 2,4-dialdehydedextran (2,4-DAXA).

Hence, instead of further increasing the H_3NSO_3 concentration, which would decrease the pH and increase the risk of side reactions, a presulfonation step was introduced, *i.e.* H_3NSO_3 was added to the solution of dialdehydedextran and the mixture stirred in the dark for several hours before the secondary oxidation was initiated, see Section *2.2*. This novel setup prioritizes the process of macromolecular chain scission over the competitive oxidative elimination of $–SO_3H$ groups during aldehyde oxidation. By changing the duration of presulfonation, M_w of DXA can be modulated between 5 and 100 % of that of DXA prepared without presulfonation, see Figure 2B. DXA derivatives with M_w between 184 kDa (prepared without presulfonation, *PDI* = 3.54) and 10 kDa (6 h of presulfonation, *PDI* = 1.43) were obtained, see Table S1 in Supporting Information. Moreover, the *PDIs* of DXA samples are significantly lower than that of source dextran (5.59) even without any additional purification steps, which is another benefit of the sulfonation-induced chain scission method. It should be noted, however, that the degree of polymerization of DXA prepared without the presence of sulfamic acid is about 37 % higher compared to source dextran polysaccharide (DP 911 vs. DP 664). This is likely caused by the formation of a dense network of rather stable intermolecular hemiacetal bonds after the periodate oxidation previously described for oxidized dextran,(Ishak & Painter, 1978; Maia et al., 2011) which may survive even through secondary oxidation. (Münster et al., 2020)

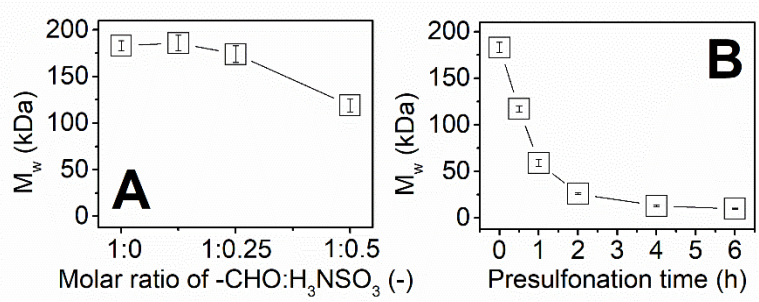

Figure 2 Weight-average molecular weight (M_w) of dicarboxydextran (DXA) prepared using A) of various molar ratios of sulfamic acid (H_3NSO_3), B) different presulfonation times (0–6 h). All measurements were performed in triplicates, error bars represent *S.D.*

Prepared materials were characterized by EDS, FT-IR, and ^{1}H NMR spectroscopy, see Supporting Information. EDS analysis confirmed the successful elimination of $–SO_3H$ groups during the secondary oxidation. The residual sulfur content was between 0.14–0.50 at% depending on the presulfonation length, see Table S2. To further reduce the amount of residual sulfur, one may decrease the concentration of H_3NSO_3 and increase the duration of secondary oxidation. (Münster et al., 2020)

The FT-IR and ^{1}H NMR spectra of species prepared using 0–6 h of presulfonation can be found in Figures S1 and S2. All FT-IR spectra are nearly identical with dominant bands belonging to vibrations of carboxylic (~1605 cm^{-1}) and C–O groups (1000–1200 cm^{-1}). The ^{1}H NMR spectra in Figure S2 are dominated by several partially overlapping signals, which position remains the same disregarding the duration of the presulfonation step. Increasing intensity of the signal at 4.14 ppm, which overlaps with signals of H4 from 2,4-dicarboxydextran (4.12 ppm) and H4 from 3,4-dicarboxydextran (4.11 ppm)(Münster et al., 2021) is attributed to the presence of an increased number of end groups in low-M_w derivatives, *i.e.* those prepared using longer presulfonation times. The degree of oxidation of all species is assumed to be ~85 % due to the presence of approximately 15 % of α-(1→3) branched units resistant to oxidation (*e.g.* signal at 3.45 ppm in Figure S2). (Khomyakov et al., 1965; Münster et al., 2021) For full signal assignment see our recent work. (Münster et al., 2021)

3.2 Cisplatin loading and release studies.

Three DXA derivatives prepared using 0, 1, and 4 h of presulfonation and having M_w of 184, 59, and 13 kDa, respectively, were selected for further studies. These were loaded by CP using 2:10, 5:10, and 8:10 CP : DXA w/w reaction ratio, see Section *2.4* for more details. CP loading effectiveness was about 90 % in all cases, resulting in 15, 30, or 45 wt% of bound CP in the conjugates (established by XRF spectroscopy). Investigated conjugates are in the following text designated by letters H, M, and L which stands for High, Medium, and Small molecular weight (184, 59, and 13 kDa), respectively, and by the number representing the amount of loaded CP in wt% (15, 30, 45). Hence, H-15 stands for DXA sample prepared without presulfonation (M_w = 184 kDa) carrying 15 wt% of CP. L-45 represents a sample with 4 h of presulfonation of M_w = 13 kDa carrying 45 wt% of CP and so on.

Cumulative drug release results of selected H-, M- and L- conjugates are given in Table S3 in Supporting Information. Here we discuss only the H- and L-series samples, where the largest differences in drug

release kinetics were observed, see Figure 3. Both M_w of the carrier and the amount of loaded CP significantly influence the CP release kinetics. Samples containing only 15 wt% of CP feature slower drug release than corresponding 45-series ones, particularly early on, see Figure 3. An increase of DXA M_w, from 13 to 184 kDa, slows down the CP release rate significantly; about 40 % less CP is released after 24 h from the H-15 sample in comparison with the L-15 sample and about 20 % less from H-45 compared to the L-45 sample, see Table S3 in Supporting Information. A combination of lower drug loading and higher M_w of the carrier leads to about 50 % slower release of CP from the H-15 sample after 24 h compared to the L-45 sample. The increased molecular weight of DXA in combination with optimization of drug loading can thus be used to (at least partially) counter the reported rapid drug release rates of DXA conjugates. (Nakashima et al., 1999)

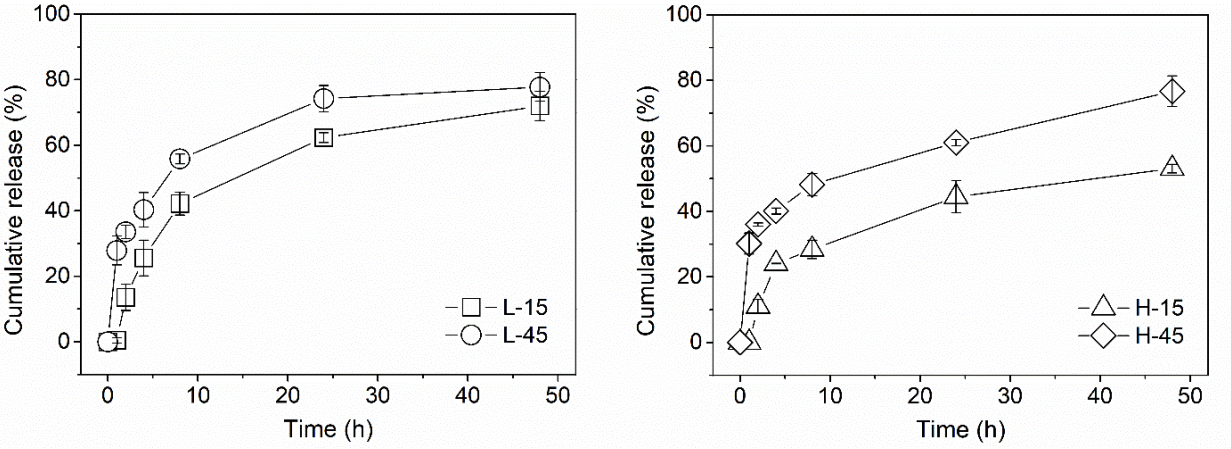

Figure 3 Cumulative release of CP from L-15, L-45, and H-15 and H-45 DXA carriers for 48 h, error bars correspond to *S.D.*

3.3 Cytotoxicity evaluations.

Cytotoxicity of the H-15, H-45, M-30, and L-15 samples was investigated by *in vitro* study on the panel of five cell lines representing three types of carcinomas often treated with CP - ovarian carcinoma represented by A2780 human cells and its CP-resistant subline A2780/CP, lung cancer represented by A549 human adenocarcinoma cells and prostate cancer represented by 22Rv1 and metastatic PC-3 human cell lines. The cytotoxicity of carriers and their conjugates was established by MTT assay, see Section *2.5*. Presented IC_{50} values (μM) are defined as a concentration of cisplatin required to inhibit the cell growth of the given cell line by 50 %. The IC_{50} values of free carriers are not provided because all carriers were non-toxic in the whole range of concentrations (up to 500 μM) and IC_{50} thus could not be calculated. It should be stressed out that reported IC_{50} values correspond to the *total* concentration of CP in a culture media (100 % release of CP from conjugates is assumed); applied doses of different conjugates were thus modified to contain the same total amount of CP as the sample of free CP. This allows to directly compare the efficacy of the free drug and individual conjugates and highlight the differences between individual carriers. The IC_{50} values are given in Tables S3 and S4 and compared in Figure 4.

Obtained IC_{50} values differ considerably between the cell lines as well as between incubation times (note different scaling on the y-axes in Figure 4). For detailed statistical analysis see Figure S3. Overall

cytotoxicity profiles of conjugates across the panel of cell lines follow that of free CP; all compounds were the most effective towards ovarian cell lines and prostatic cell line 22Rv1. Contrary, much higher doses were required to inhibit the growth of lung cancer cell line A549 as well as prostatic PC-3 cell line after 24 h of incubation. Nevertheless, differences between cytotoxicity of individual conjugates and the free drug could still be determined and benefits of CP conjugation to carriers with different M_w evaluated.

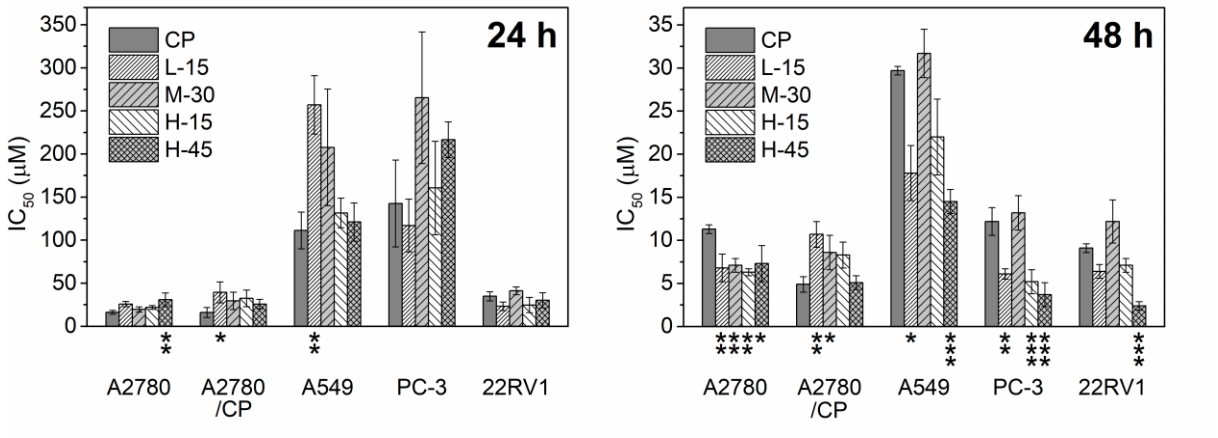

Figure 4 Comparison of IC_{50} values (μM) for free CP and CP-DXA conjugates after 24 h and 48 h of incubation with a panel of cancer cell lines. Values are the average of four independent measurements. Data are displayed as IC_{50} means ± *S.D*. The IC_{50} values of CP carriers were related to the CP IC_{50} value for each cell line and duration of treatment. Stars indicate statistical significance of the result: absent stars - not significant, *p<0.05, **p<0.01, ***p<0.001. Statistical analysis was performed using one-way ANOVA followed by Tukey *post-hoc* test.

After 24 h of incubation, cytotoxicity of all conjugates is comparable or lower than that of free CP. This is a common feature of macromolecular carriers attributable to the slower penetration of macromolecules into the cells compared to a free drug. Distinct differences between individual carriers and the free CP are, however, observable after 48 h of incubation. Notably, observed differences do not correspond to the drug release rates as one may expect. Instead, they depend on the M_w of the carrier, although the dependence is not linear. While L-15, H-15, and particularly H-45 conjugate are significantly more cytotoxic than free CP towards several cancerous cell lines, the cytotoxicity of M-30 is comparable or lower than that of free CP in 4 out of 5 cases, see Figure S3. Overall, H-45 conjugate offers the highest CP anticancer efficacy enhancement, being more effective than free drug in four out of five cases, and comparable to free CP only for A2780/CP cell line, see Figure 4. The H-45 conjugate is nearly four times more effective than free CP for both prostatic cell lines and about twice more for A2780 and A549 cell lines, see Figure 4. It is thus by far the most cytotoxic from all tested compounds, including the H-15 derivative with the same molecular weight. The effect of increased cytotoxicity due to higher CP loading is further discussed in Section *3.5* below.

3.4 Migrastatic potential

Wound healing migration assay was performed on A2780 cells, which were treated with free CP and two of the most effective conjugates, the L-15 and the H-45, which are prepared using DXAs of different molecular weights. Drug and conjugates were applied in doses corresponding to their respective IC_{50}

values determined in the previous section. Cells were incubated for 24 and 48 h, respectively, see Figure 5 and Table S5 in Supporting information. For detailed statistical analysis see Figure S4.

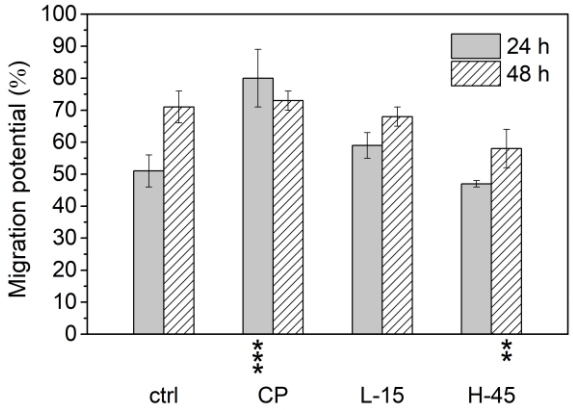

Figure 5: Migration potential of A2780 cells (%), *i.e.* the percentage of wound area covered after 24 h and 48 h by untreated cells (ctrl) and cells treated with free CP, L-15, and H-45; applied concentrations correspond to their respective IC_{50} values. All experiments were performed in triplicates; error bars correspond to *S.D*. Statistical analysis was performed using one-way ANOVA followed by Tukey *post-hoc* test with respect to untreated control; stars indicate statistical significance of the result: absent stars - not significant, **p*<0.05, ***p*<0.01, ****p*<0.001.

After 24 h of incubation with free CP, A2780 cells showed a great increase in migration potential, covering roughly 80 % of the original wound area. This is significantly more than the untreated control, see Figure 5 and representative micrographs of the wound healing assay in Figure 6. Treating the cells with CP-DXA conjugates, particularly the H-45, led to significantly better results; only between 50–60 % of the area healed after 24 h. In other words, conjugates showed a statistically significant reduction of migration potential compared to free CP (see Figure S4 for statistical comparison), although their effect on cell migration is not statistically significant when compared to the untreated cells after 24 h. There is, however, a statistically significant decrease of cell migration after 48 h treatment of A2780 cells by H-45 conjugate, when only about 60 % of wound area is healed, compared to 70–80 % in case of untreated control and free CP, respectively, see Figure 5. Once again, H-45 showed the best result from all tested compounds.

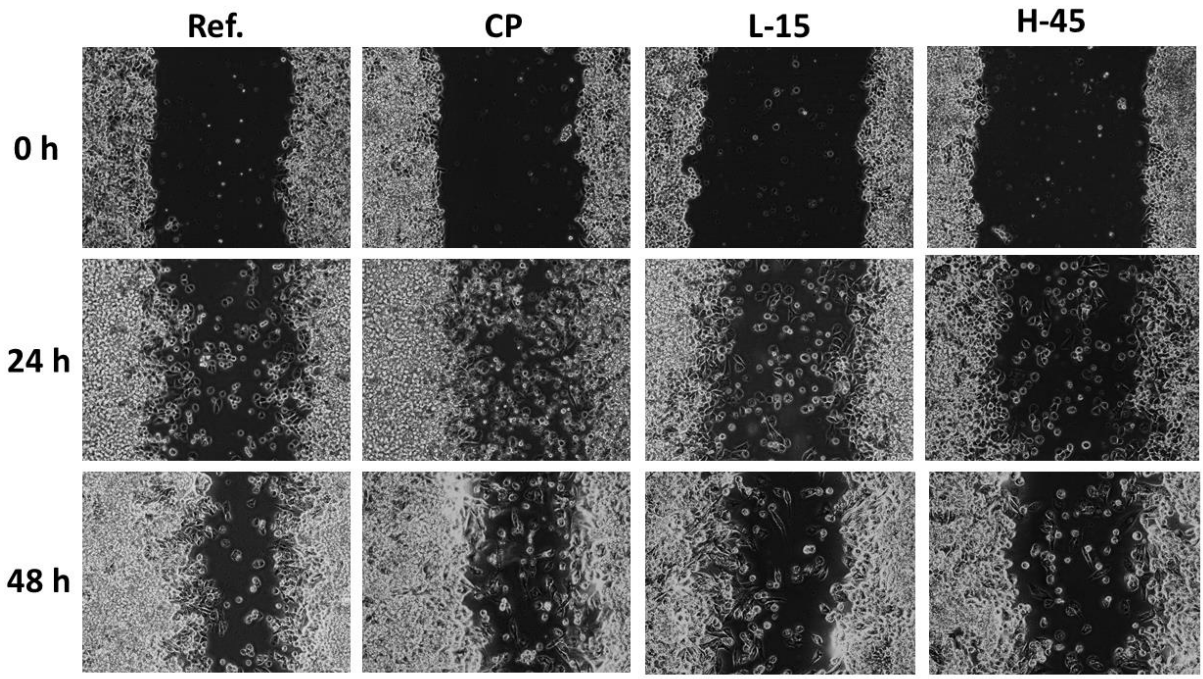

Figure 6: Micrographs of the wound healing migration assay of A2780 cell line after 0, 24, and 48 h of incubation. All compounds were applied in IC_{50} doses established previously by the MTT assay. Ref. – untreated, CP – treated with free CP, L-15 – low-M_w DXA with 15 wt% of CP, H-45 – high-M_w DXA with 45 wt% of CP.

3.5 The role of cisplatin loading to conjugate nano-assemblies

The biological evaluation revealed that the efficacy of CP-DXA conjugates depends not only on the molecular weight of DXA but also on the amount of conjugated CP. We emphasize once more that the dose of each conjugate was set to contain an equal amount of CP; the increased cytotoxic effect of H-45 conjugate thus cannot be attributed to the higher amount of CP in applied doses and the underlying reason lies elsewhere.

It is a known fact that CP can form interstrand crosslinks between the polysaccharide chains. This behavior was used to prepare CP-loaded nanoparticles (Cai et al., 2008) or nanogels (Ohta et al., 2016) in the past. Hence, a higher amount of conjugated platinum may influence characteristics of nanostructures formed by macromolecular DXA conjugates in solution, which would, in turn, alter the cell internalization and thus also the efficacy of the conjugated drug. To investigate, H-15 and H-45 conjugates, prepared using the DXA of the same M_w but with different amounts of CP, were studied by TEM and DLS analysis. Figure 7 shows the TEM micrographs of H-15 (part A) and H-45 (part B). Interestingly, both samples contain roughly similar spherical particles of approximately 3.5 ± 1 nm in diameter. Contrary, DLS measurements of hydrodynamic radii revealed significantly larger values (252 ± 8 nm for H-15 and 151 ± 9 nm for H-45). Conjugate nano-assemblies thus could be best described as nanogels, based on following reasoning: The small and rather uniform size of particles observed by TEM can be explained as a result of nanogel structure collapsing during sample drying. This process is similar for both samples because they are formed by DXA

macromolecules of the same size. Much larger hydrodynamic radii of particles measured in colloidal solutions than indicate significant swelling of both nano-assemblies in water, which is one of the main characteristics of nanogels.

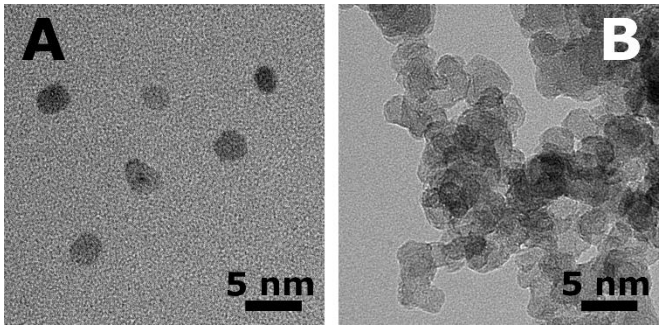

Figure 7 TEM micrographs of H-15 (part A) and L-45 (part B).

The difference in hydrodynamic radii (swelling) between H-15 and H-45 samples is then attributed to i) higher swelling due to a more sparsely crosslinked network (lower amount of loaded CP) in the H-15 sample and ii) the presence of larger ionic corona due to a higher amount of residual -COO^- groups in H-15 sample, because of the lower number of carboxyl groups being used for CP binding in H-15 than in H-45. This assumption is supported by the measured ζ-potential values (-34.2 ± 1.3 mV for H-15 and -21.3 ± 0.9 mV for L-45). The characteristics of CP-DXA nanogels thus depend on the amount of loaded CP and are likely responsible for the observed influencing of the biological properties. To further support this conclusion, the sample M-30, which showed the lowest anticancer efficacy from all tested species, has been also investigated using DLS. The M-30 nanogel particles were found to have a hydrodynamic radius of 374 ± 40 nm, more than twice the size of H-45 nanoparticles (ζ-potential = -33.7 ± 2.6 mV). This is likely a result of a combination of shorter (yet still relatively large) DXA chains, which offer fewer crosslinking spots per macromolecule than larger H-chains, and relatively low CP loading (5 : 10). Both factors thus result in a more sparsely crosslinked nanogel network compared to H-species which would also swell more significantly in solution - hence the larger size of M-30 nanogel particles. The large dimensions of the M-30 nanogel particles are also a likely reason for their poor biological efficacy, as they likely impact the cellular uptake and thus the amount of the drug that crosses the cellular membrane.

4. Conclusions

DXAs of different molecular weights had been prepared by the modification of the recently developed method for controlled chain scission of oxidized polysaccharides using sulfamic acid. This allows to advantageously use the same starting material to prepare DXA with desired M_w and decreased polydispersity (compared to source dextran). To investigate the possible gains of control over the M_w of DXA, selected derivatives with M_w between 13 and 184 kDa were loaded with 15, 30, or 45 wt% of CP, respectively, and their drug release rates, *in vitro* cytotoxicity profiles, and suppression of cancer cell migration were compared with free CP.

Increasing M_w of the carriers significantly decreases the CP release rates, and thus partially counters the main issue of DXA carriers – fast drug release rates. For instance, a high-M_w carrier with 15 wt% of CP released about 40 % less CP after 24 h than its low-M_w counterpart.

The *in vitro* cytotoxicity of CP towards malignant cell lines was enhanced by its binding to low- (13 kDa) and particularly to the high-M_w DXA (184 kDa), while its conjugation to medium-M_w DXA (59 kDa) attenuated its cytotoxicity in comparison with a free drug. Biological properties of CP-DXA conjugates are, besides the M_w of DXA, also influenced by the amount of loaded CP, which crosslinks macromolecular DXA chains into nanogels. The larger the amount of loaded CP, the denser the crosslinking. The combination of a high-M_w carrier and high drug loading (H-45 sample) led to a spontaneous formation of nanogel particles with a hydrodynamic radius of ~150 nm, which shows the highest anticancer efficacy from all tested samples. The potency of this conjugate was twice larger on average than that of a free drug across the whole panel of tested cancer cell lines and up to four times higher against both malignant prostatic cell lines. Further, H-45 conjugate showed statistically significant inhibition of the ovarian cancer cell migration when compared both to free cisplatin and untreated control. H-45 was also significantly more effective than H-15 conjugate, which is formed by the same DXA chains, yet more sparsely crosslinked (hydrodynamic radius of ~250 nm), and particularly the M-30 conjugate (hydrodynamic radius of ~375 nm), presumably because of the smaller size (and lower negative charge) of H-45 nanogel particles facilitates easier crossing over the cellular membrane.

To summarize, the study demonstrates the potential of DXA nanogels prepared using DXA of different M_w as anticancer drug carriers capable to enhance therapeutic response and suppress metastatic spreading by improving the characteristics of the drugs already established in the clinical setting. The observed relationship between biological efficacy and physical characteristics of cisplatin-crosslinked nanogel formulations is also interesting. Possibly, optimization of their parameters might improve the biological characteristics of dextran nanogels even further.

Acknowledgments

This work was supported by the Ministry of Education, Youth, and Sports of the Czech Republic – DKRVO (RP/CPS/2020/006). M. Fojtů and M. Masařík were supported by the Ministry of Education, Youth and Sports of the Czech Republic, project Advanced Functional Nanorobots reg. No. CZ.02.1.01/0.0/0.0/15_003/0000444. M. Fojtů was further supported by the start-up grant InGA/SUP/08/2020 from the Masaryk University in Brno. Z. Capáková acknowledges Czech Science Foundation grant 19-16861S. CIISB research infrastructure project LM2018127 funded by the Ministry of Education, Youth and Sports of the Czech Republic is gratefully acknowledged for the financial support of the NMR measurements at the Josef Dadok CEITEC core facility in Brno.

Associated Information

Supporting Information. Molecular weight distributions, FT-IR and ^{1}H NMR spectra of DXA derivatives; EDS analysis results; Drug-release data; IC_{50} values of CP and individual CP-DXA conjugates and their statistical analysis; Open-wound area evaluation and statistical analysis.

Author Contributions

L. Münster – Methodology, Investigation, Validation, Visualization, Writing – original Draft, Writing – review and editing. M. Fojtů – Investigation, Validation, Visualization, Formal analysis, Writing – original Draft, Writing – review and editing, F. Latečka – Investigation, M. Muchová – Investigation, Validation, Formal analysis, S. Káčerová - Investigation, Validation, Formal analysis, Z. Capáková – Investigation,

Validation, Formal analysis, T. Juriňáková - Investigation, Validation, Formal analysis, I. Kuřitka – Funding acquisition, Resources, Writing – original Draft, M. Masařík – Conceptualization, Methodology, Resources, Supervision, Funding acquisition, Writing – original Draft, Writing – review and editing, J. Vícha - Methodology, Investigation, Visualization, Writing – original Draft, Writing – review and editing, Conceptualization, Supervision, Project administration

Notes

The authors declare no competing financial interest.

References:

Ahmad, S., Tester, R. F., Corbett, A., & Karkalas, J. (2006). Dextran and 5-aminosalicylic acid (5-ASA) conjugates: Synthesis, characterisation and enzymic hydrolysis. *Carbohydrate Research*, *341*(16), 2694–2701. https://doi.org/10.1016/j.carres.2006.08.015

Annunziata, A., Amoresano, A., Cucciolito, M. E., Esposito, R., Ferraro, G., Iacobucci, I., Imbimbo, P., Lucignano, R., Melchiorre, M., Monti, M., Scognamiglio, C., Tuzi, A., Monti, D. M., Merlino, A., & Ruffo, F. (2020). Pt(II) versus Pt(IV) in Carbene Glycoconjugate Antitumor Agents: Minimal Structural Variations and Great Performance Changes. *Inorganic Chemistry*, *59*(6), 4002–4014. https://doi.org/10.1021/acs.inorgchem.9b03683

Annunziata, A., Cucciolito, M. E., Esposito, R., Ferraro, G., Monti, D. M., Merlino, A., & Ruffo, F. (2020). Five-Coordinate Platinum(II) Compounds as Potential Anticancer Agents. *European Journal of Inorganic Chemistry*, *2020*(11–12), 918–929. https://doi.org/10.1002/ejic.201900771

Bononi, G., Iacopini, D., Cicio, G., Pietro, S. D., Granchi, C., Bussolo, V. D., & Minutolo, F. (2021). Glycoconjugated Metal Complexes as Cancer Diagnostic and Therapeutic Agents. *ChemMedChem*, *16*(1), 30–64. https://doi.org/10.1002/cmdc.202000456

Cai, S., Xie, Y., Bagby, T. R., Cohen, M. S., & Forrest, M. L. (2008). Intralymphatic Chemotherapy Using a Hyaluronan–Cisplatin Conjugate. *Journal of Surgical Research*, *147*(2), 247–252. https://doi.org/10.1016/j.jss.2008.02.048

Chang, R. L., Ueki, I. F., Troy, J. L., Deen, W. M., Robertson, C. R., & Brenner, B. M. (1975). Permselectivity of the glomerular capillary wall to macromolecules. II. Experimental studies in rats using neutral dextran. *Biophysical Journal*, *15*(9), 887–906. https://doi.org/10.1016/S0006-3495(75)85863-2

Dhaneshwar, S. S., Kandpal, M., Gairola, N., & Kadam, S. S. (2006). Dextran: A promising macromolecular drug carrier. *Indian Journal of Pharmaceutical Sciences*, *68*(6), 705. https://doi.org/10.4103/0250-474X.31000

Goodarzi, N., Varshochian, R., Kamalinia, G., Atyabi, F., & Dinarvand, R. (2013). A review of polysaccharide cytotoxic drug conjugates for cancer therapy. *Carbohydrate Polymers*, *92*(2), 1280–1293. https://doi.org/10.1016/j.carbpol.2012.10.036

Haxton, K. J., & Burt, H. M. (2009). Polymeric drug delivery of platinum-based anticancer agents. *Journal of Pharmaceutical Sciences*, *98*(7), 2299–2316. https://doi.org/10.1002/jps.21611

Ishak, M. F., & Painter, T. J. (1978). Kinetic evidence for hemiacetal formation during the oxidation of dextran in aqueous periodate. *Carbohydrate Research*, *64*, 189–197. https://doi.org/10.1016/S0008-6215(00)83700-3

Khomyakov, K. P., Penenzhik, M. A., Virnik, A. D., & Rogovin, Z. A. (1965). Synthesis of dialdehydo- and dicarboxydextran. *Polymer Science U.S.S.R.*, *7*(6), 1140–1145. https://doi.org/10.1016/0032-3950(65)90394-1

Kristiansen, K. A., Potthast, A., & Christensen, B. E. (2010). Periodate oxidation of polysaccharides for modification of chemical and physical properties. *Carbohydrate Research*, *345*(10), 1264–1271. https://doi.org/10.1016/j.carres.2010.02.011

Liechty, W. B., Kryscio, D. R., Slaughter, B. V., & Peppas, N. A. (2010). Polymers for drug delivery systems. *Annual Review of Chemical and Biomolecular Engineering*, *1*(1), 149–173. https://doi.org/10.1146/annurev-chembioeng-073009-100847

Maia, J., Carvalho, R. A., Coelho, J. F. J., Simões, P. N., & Gil, M. H. (2011). Insight on the periodate oxidation of dextran and its structural vicissitudes. *Polymer*, *52*(2), 258–265. https://doi.org/10.1016/j.polymer.2010.11.058

Mehvar, R. (2000). Dextrans for targeted and sustained delivery of therapeutic and imaging agents. *Journal of Controlled Release*, *69*(1), 1–25. https://doi.org/10.1016/S0168-3659(00)00302-3

552 Mehvar, R. (2003). Recent trends in the use of polysaccharides for improved delivery of therapeutic
553 agents: Pharmacokinetic and pharmacodynamic perspectives. *Current Pharmaceutical*
554 *Biotechnology*, *4*(5), 283–302. https://doi.org/10.2174/1389201033489685
555 Mehvar, R., Robinson, M. A., & Reynolds, J. M. (1994). Molecular weight dependent tissue accumulation
556 of dextrans: In vivo studies in rats. *Journal of Pharmaceutical Sciences*, *83*(10), 1495–1499.
557 https://doi.org/10.1002/jps.2600831024
558 Münster, L., Capáková, Z., Fišera, M., Kuřitka, I., & Vícha, J. (2019). Biocompatible dialdehyde
559 cellulose/poly(vinyl alcohol) hydrogels with tunable properties. *Carbohydrate Polymers*, *218*,
560 333–342. https://doi.org/10.1016/j.carbpol.2019.04.091
561 Münster, L., Fojtů, M., Capáková, Z., Muchová, M., Musilová, L., Vaculovič, T., Balvan, J., Kuřitka, I.,
562 Masařík, M., & Vícha, J. (2021). Oxidized polysaccharides for anticancer-drug delivery: What is
563 the role of structure? *Carbohydrate Polymers*, *257*, 117562.
564 https://doi.org/10.1016/j.carbpol.2020.117562
565 Münster, L., Fojtů, M., Capáková, Z., Vaculovič, T., Tvrdoňová, M., Kuřitka, I., Masařík, M., & Vícha, J.
566 (2019). Selectively oxidized cellulose with adjustable molecular weight for controlled release of
567 platinum anticancer drugs. *Biomacromolecules*, *20*(4), 1623–1634.
568 https://doi.org/10.1021/acs.biomac.8b01807
569 Münster, L., Hanulíková, B., Machovský, M., Latečka, F., Kuřitka, I., & Vícha, J. (2020). Mechanism of
570 sulfonation-induced chain scission of selectively oxidized polysaccharides. *Carbohydrate*
571 *Polymers*, *229*, 115503. https://doi.org/10.1016/j.carbpol.2019.115503
572 Münster, L., Vícha, J., Klofáč, J., Masař, M., Kucharczyk, P., & Kuřitka, I. (2017). Stability and aging of
573 solubilized dialdehyde cellulose. *Cellulose*, *24*(7), 2753–2766. https://doi.org/10.1007/s10570-
574 017-1314-x

575 Nakashima, M., Ichinose, K., Kanematsu, T., Masunaga, T., Ohya, Y., Ouchi, T., Tomiyama, N., Sasaki, H., &
576 Ichikawa, M. (1999). In vitro characteristics and in vivo plasma disposition of cisplatin conjugated
577 with oxidized and dicarboxymethylated dextrans. *Biological & Pharmaceutical Bulletin*, *22*(7),
578 756–761. https://doi.org/10.1248/bpb.22.756
579 Ohta, S., Hiramoto, S., Amano, Y., Sato, M., Suzuki, Y., Shinohara, M., Emoto, S., Yamaguchi, H., Ishigami,
580 H., Sakai, Y., Kitayama, J., & Ito, T. (2016). Production of Cisplatin-Incorporating Hyaluronan
581 Nanogels via Chelating Ligand–Metal Coordination. *Bioconjugate Chemistry*, *27*(3), 504–508.
582 https://doi.org/10.1021/acs.bioconjchem.5b00674
583 Ohya, Y., Masunaga, T., Baba, T., & Ouchi, T. (1996a). Synthesis and cytotoxic activity of dextran carrying
584 cis-dichloro(cyclohexane-trans-l-1,2-diamine)platinum(II) complex. *Journal of Biomaterials*
585 *Science, Polymer Edition*, *7*(12), 1085–1096. https://doi.org/10.1163/156856296X00570
586 Ohya, Y., Masunaga, T., Baba, T., & Ouchi, T. (1996b). Synthesis and cytotoxic activity of dextran-
587 immobilizing platinum(II) complex through chelate-type coordination bond. *Journal of*
588 *Macromolecular Science, Part A*, *33*(8), 1005–1016.
589 https://doi.org/10.1080/10601329608010901
590 Sarwat, F., Qader, S. A. U., Aman, A., & Ahmed, N. (2008). Production & characterization of a unique
591 dextran from an indigenous Leuconostoc mesenteroides CMG713. *International Journal of*
592 *Biological Sciences*, 379–386. https://doi.org/10.7150/ijbs.4.379
593 Schechter, B., Neumann, A., Wilchek, M., & Arnon, R. (1989). Soluble polymers as carriers of cis-
594 platinum. *Journal of Controlled Release*, *10*(1), 75–87. https://doi.org/10.1016/0168-
595 3659(89)90019-9
596 Schechter, B., Pauzner, R., Arnon, R., Haimovich, J., & Wilchek, M. (1987). Selective cytotoxicity against
597 tumor cells by cisplatin complexed to antitumor antibodies via carboxymethyl dextran. *Cancer*
598 *Immunology Immunotherapy*, *25*(3). https://doi.org/10.1007/BF00199151

599 Schechter, B., Pauzner, R., Wilchek, M., & Arnon, R. (1986). Cis-platinum (II) complexes of
600 carboxymethyl-dextran as potential antitumor agents. II. In vitro and in vivo activity. *Cancer*
601 *Biochemistry Biophysics*, *8*(4), 289–298.
602 Schechter, B., Rosing, M. A., Wilchek, M., & Arnon, R. (1989). Blood levels and serum protein binding of
603 cis-Platinum(II) complexed to carboxymethyl-dextran. *Cancer Chemotherapy and Pharmacology*,
604 *24*(3), 161–166. https://doi.org/10.1007/BF00300236
605 Terry, R., Yuile, C. L., Golodetz, A., Phillips, C. E., & White, R. R. (1953). Metabolism of dextran; a plasma
606 volume expander; studies of radioactive carbon-labeled dextran in dogs. *The Journal of*
607 *Laboratory and Clinical Medicine*, *42*(1), 6–15.
608 Thorén, L. (1980). The dextrans—Clinical data. *Developments in Biological Standardization*, *48*, 157–167.
609 Varshosaz, J. (2012). Dextran conjugates in drug delivery. *Expert Opinion on Drug Delivery*, *9*(5), 509–523.
610 https://doi.org/10.1517/17425247.2012.673580
611 Vilar, G., Tulla-Puche, J., & Albericio, F. (2012). Polymers and drug delivery systems. *Current Drug*
612 *Delivery*, *9*(4), 367–394. https://doi.org/10.2174/156720112801323053
613 Wilson, J. J., & Lippard, S. J. (2014). Synthetic Methods for the Preparation of Platinum Anticancer
614 Complexes. *Chemical Reviews*, *114*(8), 4470–4495. https://doi.org/10.1021/cr4004314
615